Real-Time Detection of Diabetic Retinopathy Using Deep Learning Techniques

Irfan Ali Bhacho[1], Hina Lilaram[1], Sarmad Talpur[1], Madeha Memon[*1], Nouman Qadeer Soomro[2]
[1]Department of Computer Systems Engineering (Mehran University of Engineering and Technology, Jamshoro, Sindh, Pakistan).
[2]Department of Software Engineering (Mehran University of Engineering and Technology, SZAB Campus, Sindh, Pakistan).
[*]**Correspondence:** madeha.memon@faculty.muet.edu.pk

Citation | Bhacho. I. A, Lilaram. H, Talpur. S, Memon. M, Soomro. N. Q, "Real-Time Detection of Diabetic Retinopathy Using Deep Learning Techniques", IJIST, Vol. 6 Issue. 4 pp 1848-1861, Nov 2024
Received | Sep 30, 2024 **Revised |** Oct 30, 2024 **Accepted |** Oct 31, 2024 **Published |** Nov 2, 2024.

Diabetic retinopathy is a prevalent disease which is a medical condition frequently caused due to high sugar levels in the blood. It deteriorates the optic nerve as it compresses and blurs the vision, which is used to detect white light and transmit signals to your cerebrum using a nerve. There has been a massive increase in the statistics having diabetic retinopathy which causes the loss of sight in any age group with no treatment Every diabetic patient is required to visit their ophthalmologist every two weeks or mandatorily in a month. Moreover, a bi-annual inspection is required to notice the amount of vision to see the objects. For this reason, Pakistan lacks ophthalmologists who are experts in their domain. Mostly, they are not available around the clock, especially in less privileged areas. Therefore, we have developed a smartphone-based handheld AI-integrated product that is cost-effective and portable which detects visual Impairment and produces reports of the concerned patient with a minor intervention on the same day by an eye specialist. This research project focuses on diabetic retinopathy detection by utilizing a 20D (20 Diopter) Lens and camera of any random smartphone that captures fundus images which are further spitted and compared against various models of deep learning. In this research, VGG-15, ResNet50, and Custom CNN were undertaken. As a result, VGG16 outperformed other models by obtaining the highest validation accuracy which is 74.53% as well as the lowest validation loss of 55.94%. Moreover, ResNet50 yielded 74.08% validation accuracy and a computing validation loss of 58.72%. Consequently, the custom CNN Model achieves 57.26% validation accuracy and 57.26% validation loss. Thus, VGG16 performed best on the dataset provided and is deployed in the smartphone application which is a portable and cost-effective method for Diabetic Retinopathy screening in less privileged areas. This project aims to target three Sustainable Development Goals including Affordable and clean energy, good health and well-being, and Industry Innovation and Infrastructure respectively.

Keywords: Diabetic Retinopathy, Diabetes Mellitus VGG-16, ResNet50, Custom CNN Model.

Introduction:

The World Health Organization (WHO) identifies diabetes as the tenth foremost cause of mortality worldwide. The prevalence of diabetes has been rapidly increasing in low and middle-income countries than in high-income countries [1]. Diabetic retinopathy (DR) is a condition associated with diabetes that arises when elevated blood glucose levels inflict damage on the retina, the light-sensitive tissue located at the posterior of the eye. Diabetic retinopathy (DR) impairs the retina, resulting in aberrant blood vessel proliferation that may culminate in thrombosis or rupture, as depicted in Figure 1. DR can cause blindness if left undiagnosed and untreated, making it one of the leading causes of blindness worldwide accounting for more than 3.9 million. [2] However, it takes several years for diabetic retinopathy to reach a stage where it could threaten the sight of a diabetic patient. Most patients remain asymptomatic until they reach advanced stages of DR. The available treatments including Vitrectomy and injecting medicines to the eye for visual impairment caused by diabetes have been more effective at slowing visual loss than reversing visual impairment. Therefore, the early identification of diabetic retinopathy before irreversible visual loss is essential for optimizing patient health [3].

Diabetes:

Diabetes, also referred to as diabetes mellitus (DM), is a chronic disorder that arises when the pancreas produces inadequate insulin or when the body fails to effectively utilize the insulin it produces. In 2019, diabetes resulted in 1.5 million fatalities, with 48% of the deceased being individuals under the age of 70. One in every three patients with diabetes mellitus develop DR [4]. The three major types of diabetes mellitus are type 1, type 2, and gestational diabetes.

Diabetic Retinopathy:

Diabetes-induced fluctuations in blood glucose levels cause modifications in the retinal blood vessels, culminating in a vision-threatening condition termed diabetic retinopathy (DR), characterized by vessel swelling and leakage, which leads to macular edema. Occasionally, the retinal surface may form abnormal blood vessels. These blood arteries may become dilated, potentially resulting in thrombosis and hemorrhages in the posterior segment of the eye. In the absence of treatment and thorough annual evaluation, this illness can progress substantially from mild retinopathy to vision impairment, potentially culminating in permanent blindness. Other eye conditions such as glaucoma and cataracts have a higher chance to be developing in individuals suffering from diabetes compared to the rest of the healthy population [4].

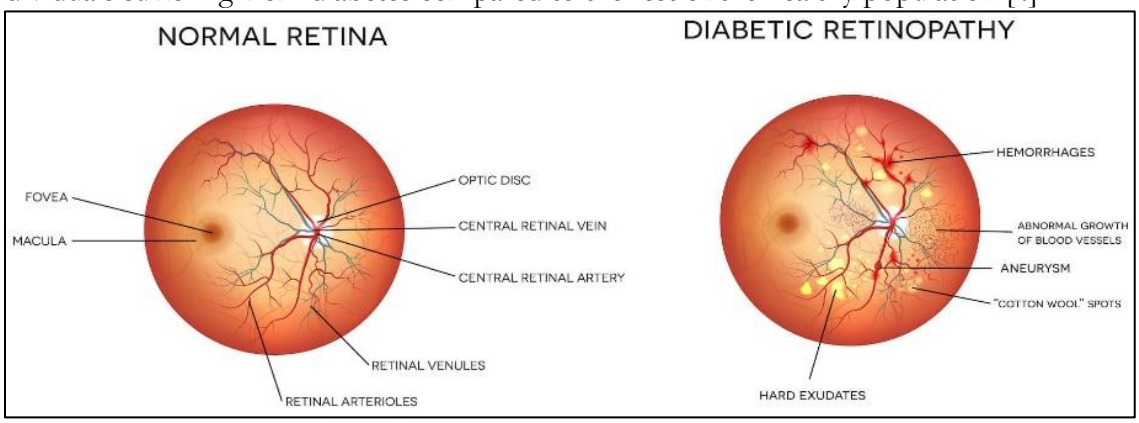

Figure 1. Comparing Normal and DR infected Eye [2]

The authors of this research have focused on four different severity levels of Diabetic Retinopathy listed below.

Literature Review:

Approximately 2.2 billion individuals globally experience distant or near vision impairment including visual damage that either has been avoided or is still unaddressed and untreated [2]. According to records of Asia [5], this disease develops over a period exceeding 20 years; 60% of persons with type II diabetes and nearly all individuals with type I diabetes will experience diabetes during their lifetime [6].

The researchers [7][8] integrated single-field imaging, demonstrating that the optic nerve and macula are discernible in single-field fundus imaging within a 20–50-degree visual field. In 1991, seven standardized 30-degree ocular pictures from the Early Treatment Diabetic Retinopathy Study (ETDRS) became the industry standard for diagnosing Diabetic Retinopathy (DR) [7], which are used in Vitrectomy traditional methods. Montage images exhibited efficacy in diabetic retinopathy identification and classification, but the collection process is laborious and time-consuming. Over fifty percent of the time, peripheral lesions occur outside the typical ETDRS fields; hence, lesions aid in the detection of DR.

The OCT methodology demonstrates advanced optical sectioning capabilities, unconfined by spatial or depth resolutions [9]. It allows for accurate noninvasive examination for diabetic retinopathy, enabling patients to get treatment before experiencing irreparable visual loss. This method analyses cross-sections of tissues by employing low-coherence light and analyzes the reflections produced from tissue surfaces. OCT-angiography used for DR detection and monitoring may benefit from several OCT-Angiography (OCTA) measurements [10]. To standardize these metrics, it is essential to establish parameters that mitigate the impact of extraneous variables such as age, comorbidities, and duration of diabetes. A non-invasive alternative to fluorescein angiography for Diabetic Retinopathy detection is provided by the OCT-angiography examination, due to which generates a lot of interest for research opportunities and examination [11].

Matching Filtering (MF) and bilinear top-hat screening are used in [12], and results are subsequently provided to a region-growing algorithm. Other publications, such as wavelet transform in [13] and radon transform in [5], convert image-based characteristics to a different space. Many of these algorithms have produced an accuracy of around 79% while still being computationally economical, however, such simplistic designs are susceptible to functional issues. Many essential characteristics, such as microaneurysms and hemorrhages, might be inaccurately detected using intensity-based methods. SVMs were used by [14][15] to find blood vessels and locate PDR instances. A study in [16] focuses on finding microaneurysms (MAs) by implementing an SVM-based ensemble model structure, multi-model medium, and Gaussian Mixture Models (GMM). The authors in [9] proposed a method where SVM assigned a grade of DR and tracked changes in red lesions. This method facilitates swift class differentiation and intricate feature representations; nonetheless, it still necessitates some human involvement, which may result in errors in challenging tasks [17]. A likelihood distribution normalization and the K-Nearest Neighbors (KNN) algorithms were implemented by [18][19]. The study in [20] generates splattered partitions after dividing fundus images, it selects the best features using a filter and a wrap-per sequence, then implements a KNN model to classify possible hemorrhages. KNN performs well across tasks as a general-purpose classifier, although it may have problems with computing efficiency and generalizability. Therefore, training on new data across various population applications or retaining extremely big training data would be required for distinct patient groups. Based on RFs, [21][22] detect binary DR. RFs can also distinguish between lesions and non-lesions thanks to candidate morphology, according to [23]. This technique can provide obvious class distinctions, but it involves manual work and may have problems with less defined class boundaries (i.e. mild from moderate). Particle Swarm Optimization (PSO) was used by [24] to extract characteristics from retinal pictures, which were then input to an NN to categorize DR.

Research Methodology:

The research process began with data collection using a specific device, followed by preprocessing to eliminate outliers. This cleaned data was then used to train a model based on a 20D lens, which had not been publicly available before. Consequently, we acquired information through real-time imaging of OPD patients, facilitated by the Sindh Institute of Ophthalmology and Visual Sciences Hospital in Hyderabad (SIOVS). The data was labeled and graded with the help of ophthalmologists at the supporting hospital which proved to be ground truth evidence.

Dilation:

The patient's eye is fully dilated using dilating drops prescribed by the ophthalmologists before capturing the image for the fundus to be visible as depicted in Figure 5.

Device Design:

This device is a handheld fundoscopic that can be used by a trained ophthalmologist or anyone with minimal training to capture images. A complete device is depicted in Figure 2.

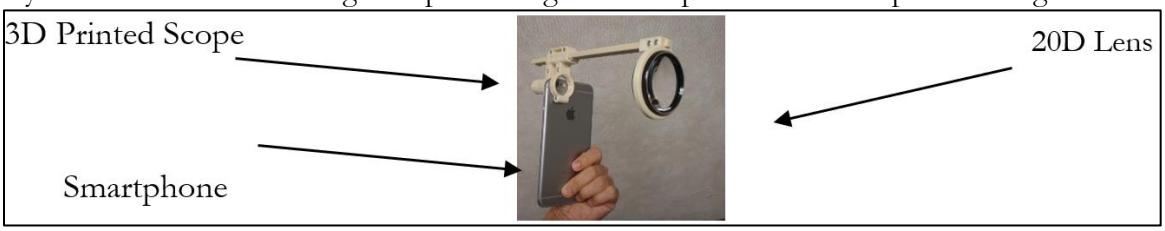

Figure 2. Complete Device

20D Lens:

The 20D lens is used for general examination of the fundus. This provides a high-resolution image of the retina in the OPD or the operating room. A 45-degree field of view helps in visualization up to the mid-peripheral region. The 3D scope is adapted from the Odocs eye care open-source 3D printing source. It is the world's first open-source retinal imaging adaptor called the Ophthalmic Docs Fundus. It is used to perform indirect ophthalmoscopy using a smartphone and a 20D lens. This device converts a smartphone into a fundus camera that can capture images of the retina.

Smartphone:

Images of the fundus were taken using an Android smartphone with OS Version 6 or above. The smartphone is attached to one end of the 3D scope and the other end is fixed with a 20D lens. We opened the camera (preferably in video mode with flash/torch option on) and focused the retina to the center of the camera to capture a clear image or record a video from which the image was extracted later on.

Mechanism of Device:

- To get rid of any debris, thoroughly clean the 20D lens and the smartphone camera lens before the process. The slots at the ends of the 3D scope gadget were used to hold a smartphone with a Volk 20D lens.
- The gadget is held around 3-5 cm in front of the patient's eye. Once the fundus of the eye is visible and clear in the camera, the image is captured or a video is recorded from the smartphone screen, the flash option is activated throughout this process for a consistent light source.
- The gadget was slightly tilted or moved back and forth to do this, and an infant depressor was used to stabilize the patient's eyes. Additionally, good mydriasis reduced reflections.
- After the recording was completed, the high-quality snapshots that were obtained were extracted from the video frames using the smartphone's screenshot capability.
- Classification of snapshot photos using DR, the photographs were then uploaded to a smartphone application.

Dataset Description:

The fundus image data was collected from the Sindh Institute of Ophthalmology and Visual Sciences (SIOVS) Hyderabad hospital and merged with an open-source Kaggle competition data for the detection of diabetic retinopathy [25]. In total, the dataset comprised 35,122 images divided into two classes: DR and No-DR. 9,313 images were DR fundus and 25,809 images were No DR fundus. In this study, we detected DR using a 20D (Diopter) ophthalmic Lens and a smartphone-based camera to capture fundus images of 150 OPT patients at the SIOVS hospital. These images were used to test the deep learning model based on CNN, VGG16. A dataset of 10,000 fundus images acquired from a fundus camera operating at the hospital was used to train the model and 150 images captured from a 20D lens were used to test the model. The results were classified into two categories namely (DR and no DR) that were compared against the three deep learning models. A Publicly available Kaggle dataset EyePACS [25] was merged with the dataset obtained from the SIOVS hospital. Three components area of exudates, the area of blood vessels, and the area of the microaneurysm have been used to classify the samples. We divided the conditions into two categories: DR and NO DR.

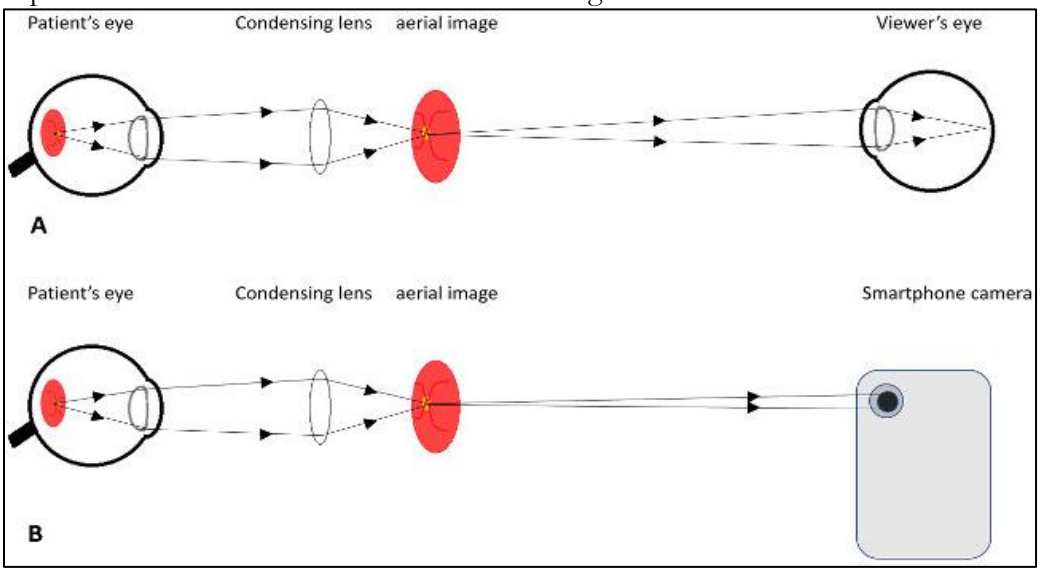

Figure 3. Image Acquisition Process

Preprocessing:

The open-source data was collected from different sources it had a lot of differences in the images. Some were zoomed in, and some zoomed out. The ratio of the fundus of an eye to an image had to be set the same for all images. Thus, we created a Python script to accomplish the preprocessing of all images cut the extra black background of all the images, and set the standard resolution for all images, i.e., 300*300.

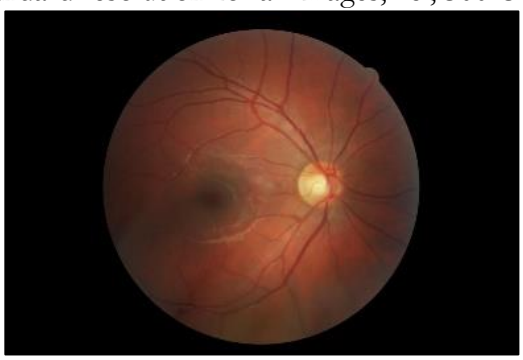

Figure 4. (a) Before Preprocessing

Figure 4. (b) After Preprocessing

The dataset was split into 790 images from the data for validation. Later, we divided the rest of the data into 80% training dataset and 20% validation dataset.

Deep Learning Algorithms:

ImageNet Large Scale Visual Recognition Challenge:

Three different deep learning algorithms were incorporated along with transfer learning to train our model. ImageNet Large Scale Visual Recognition Challenge (ILSVRC) is an annual worldwide deep learning competition that evaluates algorithms developed on the ImageNet dataset that has a variety of classes, for image classification and object detection. The algorithms used below are the top-performing algorithms from ILSVRC. These algorithms can outperform almost every dataset with a bit of fine-tuning.

Convolutional Neural Network (CNN):

As the focus of this research is based on the classification of diabetic retinopathy images, we used Convolutional Neural Network algorithms, which is a Deep Learning algorithm. The reason to focus on CNNs is that they compete dominant in object detection and image classification problems.

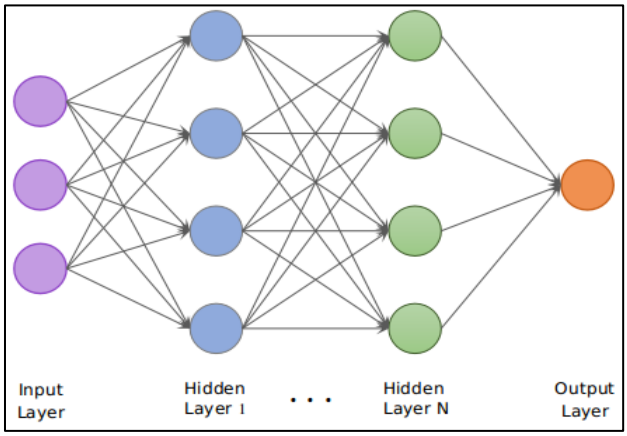

Figure 5. Basic CNN Architecture

VGG16:

VGG16 is a 16-layer CNN algorithm that achieved success in the ImageNet competition on the classification of images and detection of objects in 2014. VGG16 consists of 16 layers having weights, out of which 13 are convolution layers, and 3 are Dense layers. 5 Max Pooling Layers are used that do not hold weights.

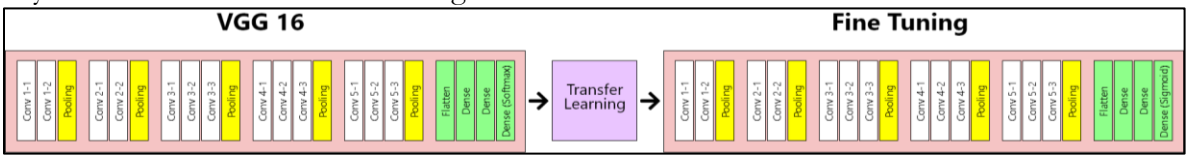

Figure 6. Fine-tuned VGG16 Architecture

VGG16 model accepts a tensor of size 224*224 with 3 RGB channels. Conv-1 Layers have a filter size of 64, Conv-2 filter size is 128, Conv-3 has 256 filters and Conv-4 and Conv-5 consist of 512 filters. The dataset in image data generator was utilized and data augmentation was performed to increase the data size as well as performed preprocessing on images for better results on the algorithm used. Moreover, VGG-16 was fine-tuned. The default output Dense layer was removed and a new Dense output layer to predict from 2 classes (DR or No DR). The sigmoid activation function was used at the output layer. The model was compiled using 'Adam' optimizer with a default learning rate i.e., 0.001, and the 'binary_crossentropy' loss function. Early stopping callback was used in the training process by monitoring validation accuracy, which means if validation accuracy doesn't seem to improve after a certain number of epochs the training process will end. We also used the restoration of

weights property on early stopping to use the weights from the epoch performing best on validation data.

Custom CNN Model:

A deep learning model with 16 layers is created; out of which seven are convolutional layers, three are pooling layers, the first layer is a flattening layer, the second layer is dropout layers, and the third layer is a dense layer.

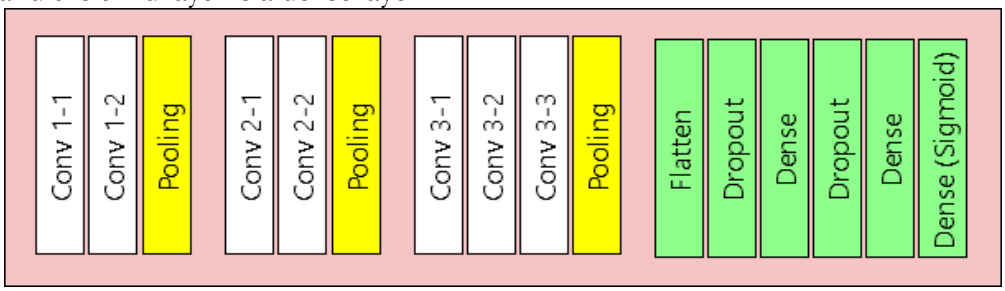

Figure 7. Custom Model Architecture

The model is directed to accept an input image of size 224 * 224. According to the Figure 7, Conv 1 layers use 64 filter size with kernel size 3. Conv 2 uses 128 filters with a 3 * 3 kernel size. Conv 3 uses a filter size of 256 with kernel size 3. For all max-pooling layers, a pool size and stride size of 2 were utilized. Dropout layers were used with a factor of 0.3. The last dense layer was used for classification, and it uses the sigmoid activation function. All the Convolutional layers were used with the same padding i.e., the image size didn't reduce due to convolution operation. The dataset was prepared using an image data generator. Furthermore, image data augmentation was conducted on train and validation data, compiled the model using 'Adam' optimizer. Additionally, the 'binary_crossentropy' loss function was calculated. For efficient training early stopping was used by checking the improvement in validation accuracy and also defined to restore the best weights. We trained the model on training data and validated it on the validation dataset using 200 epochs and early stopping callback. The CNN architecture addresses imbalanced data by utilizing various techniques, including translation invariance, parameter sharing, and pooling layers for dimensionality reduction.

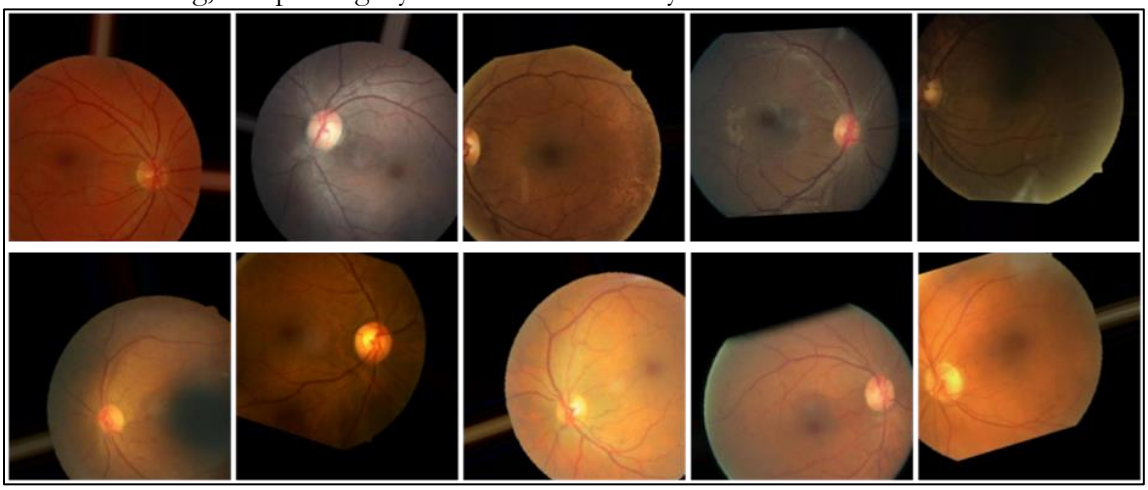

Figure 8. Sample image

User Interface of Mobile Application

An Android phone with OS Version 6 or higher may be used to take wide-angle digital color photos of the retina (fundus) using this mobile application built on the Android OS. This application is a hybrid device made up of a smartphone app and a 3D-printed scope with an indirect ophthalmoscopic lens attached. The objective of this application is to capture pictures of the retina of the eye for general viewing and patient education. With the aid of this application, the consultant may easily and swiftly take fundus photos for patient education and examination.

It helps doctors and patients have talks about how the condition is progressing and the best course of action.

Image Sharing Flow:

Figure 9. Block diagram illustrating the flow of Application.

The flow of diabetic retinopathy application is enlisted using the below steps:

- The user selects the camera to capture images. Additionally, provides access to select images from the gallery as represented in Figure 10.
- The user attaches the 3D scope to the smartphone and adjusts the camera position so that the fundus of the patient is at the center of the camera.
- After the capture of multiple images, the user will then select clear fundus images for further sharing.
- The user answers some questions regarding the patient's eye history and examination.
- The user selects the consultant and shares the examination data.

Automated Report Generation Flow:

- AI report generated; the user will select the generated a report option from the Home Screen. Figure 10.
- The user opens the camera or selects images from the gallery and uploads them to the application.
- Furthermore, the user checks the patient information for patient records and clicks on generate the report.

Tools and Technologies:

To perform the experiments for the classification of Diabetic Retinopathy using the Deep learning approach, AWS cloud computing was used to deploy Machine Learning service and Google COLAB Pro configuration as an experimental setup.

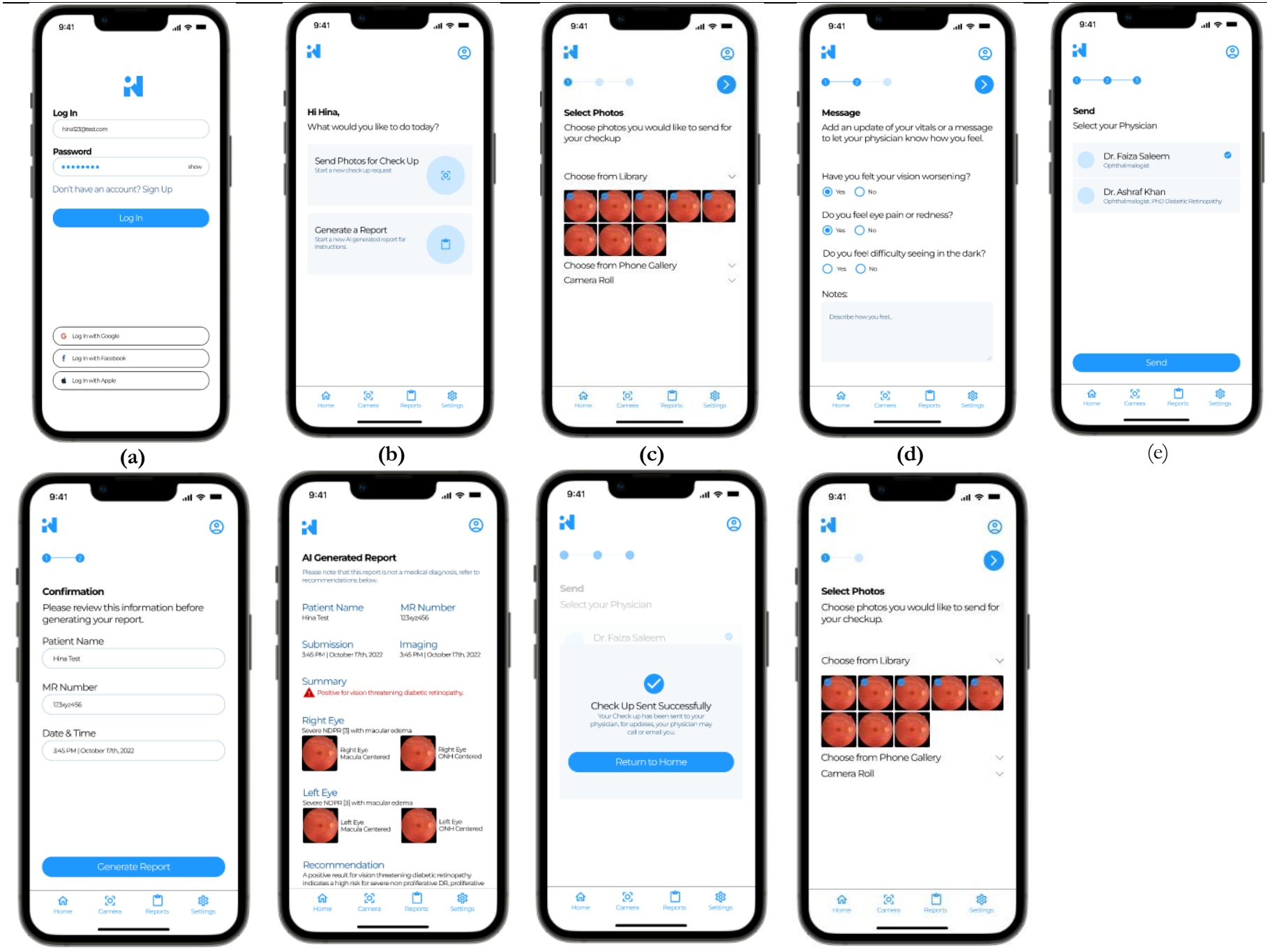

Figure 10. Diabetic Retinopathy Application Screens (a) Login (b) Home Screen (c) Image Selection (d) Questionnaire Dashboard (e)Consultant Selection (f) Message Sent Prompt (g) Select Images for AI Report (h) Confirmation Screen (i) AI-Generated DR Report

Results and Discussion:

After performing various deep learning frameworks on the image dataset of Diabetic Retinopathy, the obtained results are reviewed in this section for further comparative analysis.

VGG16:

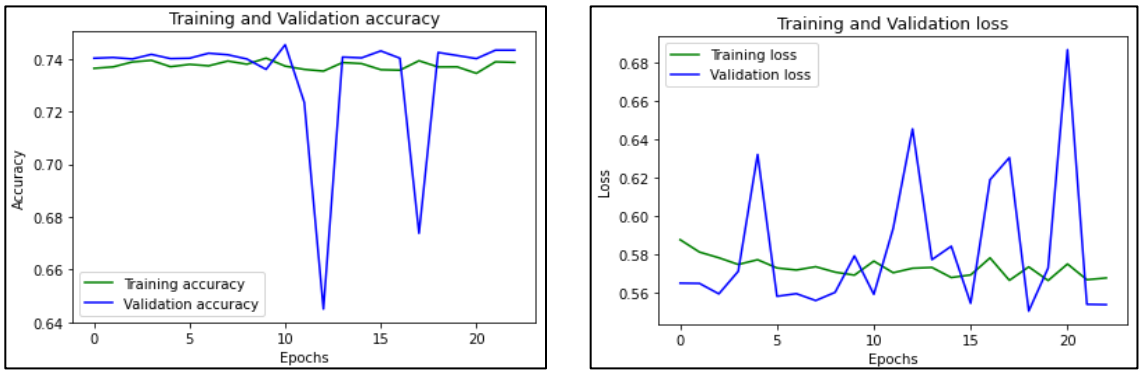

(a) **(b)**

Figure 11. (a) Represents Training and Validation Loss (b)Training and Validation Accuracy

The VGG16 Model was trained on 100 epochs. On approaching the 23rd epoch the model validation accuracy remained constant and did not improve. Therefore, the training process was stopped due to early stopping callback. Configurations and weights were restored from optimal epoch i.e. epoch 11 and batch size of 32.

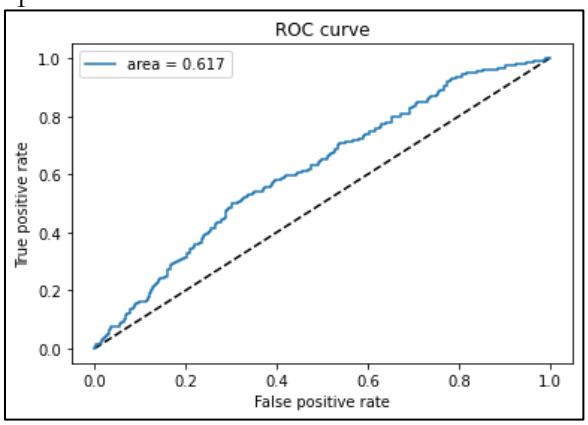

Figure 12. Highlights the ROC Curve of VGG16

Area Under the Curve (AUC) refers to the level or measurement of separability, and Receiver Operating Characteristics (ROC) is a probability curve. True Positive Rate (TPR) or recall or sensitivity is plotted against False Positive Rate (FPR) or specificity on the ROC curve, with FPR on the x-axis and TPR on the y-axis as shown in Figure 12.

ResNet50:

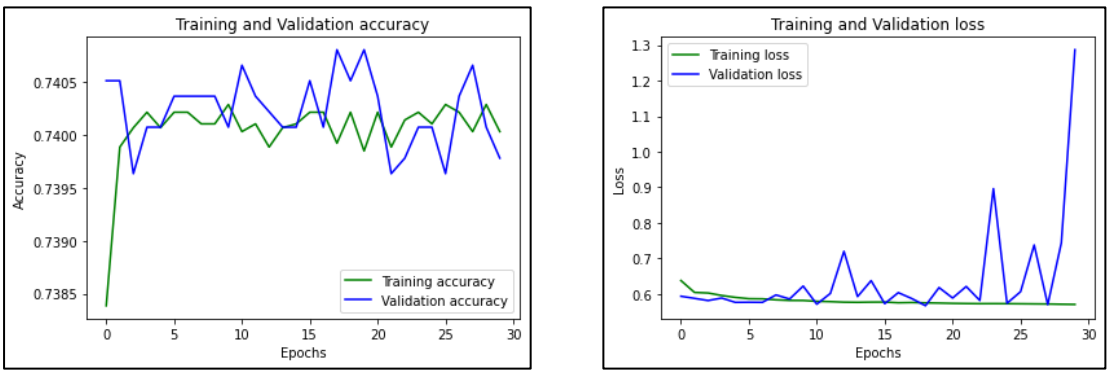

(a) **(b)**

Figure 13. (a) Training and Validation Loss, (b) Training and Validation Accuracy

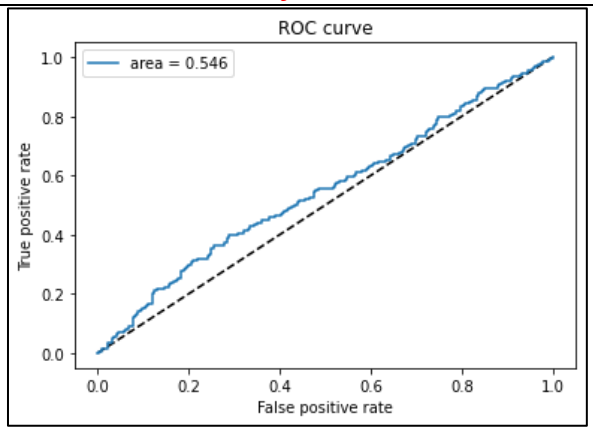

Figure 14. ROC Curve- ResNet50

After 30 epochs model training stopped with a callback of early stopping. Validation accuracy didn't improve for a few epochs and callback interrupted the training. The best model weights were restored from epoch 18 as represented in Figures 13 and 14.

Custom CNN Model:

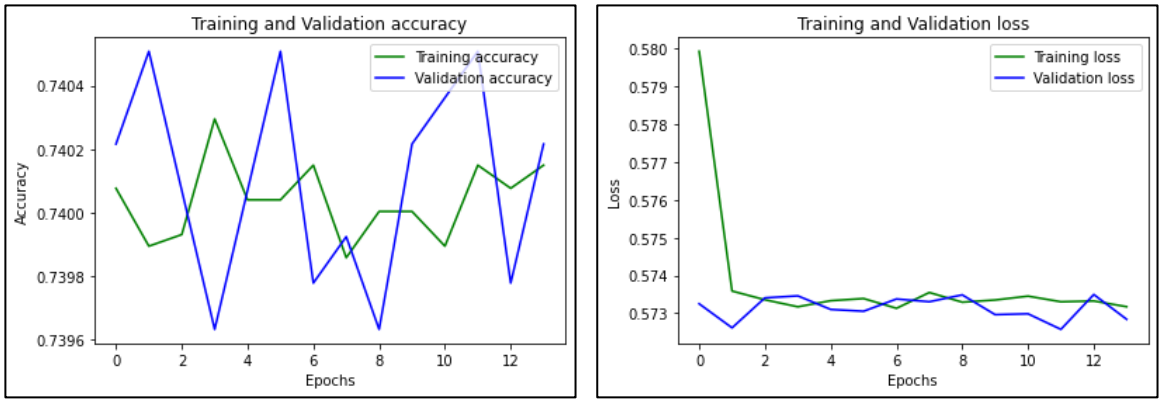

(a) **(b)**

Figure 15. (a) Training and Validation Loss, (b)Training and Validation Accuracy

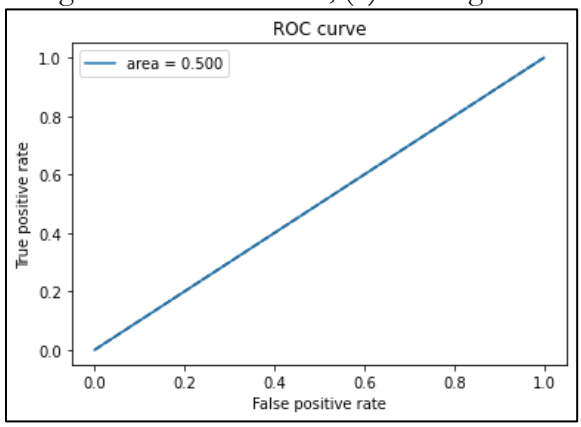

Figure 16. ROC Curve- Custom CNN Model

On approaching the 14th epoch Model training occurred successively till 14 epochs. After the 14th epoch, the model training model was stopped due to early stopping callback on approaching the highest validation accuracy. Additionally, the model weights from epoch 2 due to optimal performance as represented in Figures 15 and 16 respectively.

Comparative Analysis:

After comparing the results of all the trained deep learning models, VGG16 outperformed another model by obtaining the highest validation accuracy i.e., 74.53% as well as

the lowest validation loss of 55.94%. Thus, VGG16 performed best on the dataset provided and is deployed in the smartphone application. Moreover, ResNet50 yielded 74.08% validation accuracy and a computing validation loss of 58.72%. Consequently, the custom CNN Model achieves 57.26% validation accuracy and 57.26% validation loss.

Table 1. Comparative Analysis of VGG16, ResNet50, Custom CNN Model

Model	Training Accuracy	Training Loss	Validation Accuracy	Validation Loss	AUC	Precision	Recall	F1 Score
VGG16	0.7372	0.5767	0.7453	0.5594	0.6174	0.79	0.78	0.75
ResNet50	0.7399	0.5762	0.7408	0.5872	0.5464	0.77	0.79	0.74
Custom CNN Model	0.7399	0.5736	0.7405	0.5726	0.5010	0.74	0.75	0.77

Conclusion:

The existing systems and approaches for the detection of Diabetic Retinopathy using Smartphone-Based photography with a 20D lens or Fundus on a phone Photography, therefore, it is concluded that our proposed Diabetic Retinopathy detection technique is successful in detecting Diabetic Retinopathy. Our proposed method classifies Diabetic Retinopathy disease into two classes, namely DR (Patient has Diabetic Retinopathy) and NO DR (Patient is healthy).

Future Recommendations: A larger dataset with direct ophthalmic 20D images needs to be constructed for training data using deep learning frameworks to obtain optimum accuracy. Dataset images need to be labeled using expert opinion and must have consistent and high resolution. Additionally, dataset image frames must be kept identical. With more good resolution training data obtained from a 20D lens, the accuracy can be increased and an efficient and robust system can be developed to diagnose Diabetic Retinopathy.

Acknowledgment: We extend our gratitude to Mehran University of Engineering and Technology (MUET), Jamshoro, for offering a supportive research environment and ongoing encouragement, which enabled the successful completion of this research project.

References:

[1] Y. Kang, Y. Fang, and X. Lai, "Automatic Detection of Diabetic Retinopathy with Statistical Method and Bayesian Classifier," *J. Med. Imaging Heal. Informatics*, vol. 10, no. 5, pp. 1225–1233, Feb. 2020, doi: 10.1166/JMIHI.2020.3025.

[2] M. Ashraf, P. L. Nesper, L. M. Jampol, F. Yu, and A. A. Fawzi, "Statistical Model of Optical Coherence Tomography Angiography Parameters That Correlate With Severity of Diabetic Retinopathy," *Invest. Ophthalmol. Vis. Sci.*, vol. 59, no. 10, pp. 4292–4298, Aug. 2018, doi: 10.1167/IOVS.18-24142.

[3] C. H. Tan, B. M. Kyaw, H. Smith, C. S. Tan, and L. T. Car, "Use of smartphones to detect diabetic retinopathy: Scoping review and meta-analysis of diagnostic test accuracy studies," *J. Med. Internet Res.*, vol. 22, no. 5, 2020, doi: 10.2196/16658.

[4] G. U. Parthasharathi, K. Vasantha Kumar, R. Premnivas, and K. Jasmine, "Diabetic Retinopathy Detection Using Machine Learning," *J. Innov. Image Process.*, vol. 4, no. 1, pp. 26–33, May 2022, doi: 10.36548/JIIP.2022.1.003.

[5] S. Stolte and R. Fang, "A survey on medical image analysis in diabetic retinopathy," *Med. Image Anal.*, vol. 64, p. 101742, 2020, doi: 10.1016/j.media.2020.101742.

[6] W. L. Alyoubi, W. M. Shalash, and M. F. Abulkhair, "Diabetic retinopathy detection through deep learning techniques: A review," *Informatics Med. Unlocked*, vol. 20, p. 100377, Jan. 2020, doi: 10.1016/J.IMU.2020.100377.

[7] R. E. Hacisoftaoglu, M. Karakaya, and A. B. Sallam, "Deep learning frameworks for diabetic retinopathy detection with smartphone-based retinal imaging systems," *Pattern Recognit. Lett.*, vol. 135, pp. 409–417, Jul. 2020, doi: 10.1016/J.PATREC.2020.04.009.

[8] I. Odeh, M. Alkasassbeh, and M. Alauthman, "Diabetic Retinopathy Detection using

Ensemble Machine Learning," *2021 Int. Conf. Inf. Technol. ICIT 2021 - Proc.*, pp. 173–178, Jul. 2021, doi: 10.1109/ICIT52682.2021.9491645.

[9] R. Rajalakshmi, V. Prathiba, S. Arulmalar, and M. Usha, "Review of retinal cameras for global coverage of diabetic retinopathy screening," *Eye 2020 351*, vol. 35, no. 1, pp. 162–172, Nov. 2020, doi: 10.1038/s41433-020-01262-7.

[10] T. Spencer, J. A. Olson, K. C. McHardy, P. F. Sharp, and J. V. Forrester, "An image-processing strategy for the segmentation and quantification of microaneurysms in fluorescein angiograms of the ocular fundus," *Comput. Biomed. Res.*, vol. 29, no. 4, pp. 284–302, 1996, doi: 10.1006/cbmr.1996.0021.

[11] A. Soni and A. Rai, "A Novel Approach for the Early Recognition of Diabetic Retinopathy using Machine Learning," *2021 Int. Conf. Comput. Commun. Informatics, ICCCI 2021*, 2021, doi: 10.1109/ICCCI50826.2021.9402566.

[12] X. Zhang *et al.*, "Exudate detection in color retinal images for mass screening of diabetic retinopathy," *Med. Image Anal.*, vol. 18, no. 7, pp. 1026–1043, 2014, doi: 10.1016/j.media.2014.05.004.

[13] L. Tang, M. Niemeijer, J. M. Reinhardt, M. K. Garvin, and M. D. Abramoff, "Splat feature classification with application to retinal hemorrhage detection in fundus images," *IEEE Trans. Med. Imaging*, vol. 32, no. 2, pp. 364–375, 2013, doi: 10.1109/TMI.2012.2227119.

[14] R. A. Welikala *et al.*, "Automated detection of proliferative diabetic retinopathy using a modified line operator and dual classification," *Comput. Methods Programs Biomed.*, vol. 114, no. 3, pp. 247–261, May 2014, doi: 10.1016/J.CMPB.2014.02.010.

[15] K. A. Goatman, A. D. Fleming, S. Philip, G. J. Williams, J. A. Olson, and P. F. Sharp, "Detection of new vessels on the optic disc using retinal photographs," *IEEE Trans. Med. Imaging*, vol. 30, no. 4, pp. 972–979, Apr. 2011, doi: 10.1109/TMI.2010.2099236.

[16] E. Treatment and D. Retinopathy, "Grading Diabetic Retinopathy from Stereoscopic Color Fundus Photographs—An Extension of the Modified Airlie House Classification: ETDRS Report Number 10," *Ophthalmology*, vol. 98, no. 5, pp. 786–806, 1991, doi: 10.1016/S0161-6420(13)38012-9.

[17] W. Zhang *et al.*, "Automated identification and grading system of diabetic retinopathy using deep neural networks," *Knowledge-Based Syst.*, vol. 175, pp. 12–25, 2019, doi: 10.1016/j.knosys.2019.03.016.

[18] K. M. Adal, P. G. Van Etten, J. P. Martinez, K. W. Rouwen, K. A. Vermeer, and L. J. Van Vliet, "An automated system for the detection and classification of retinal changes due to red lesions in longitudinal fundus images," *IEEE Trans. Biomed. Eng.*, vol. 65, no. 6, pp. 1382–1390, 2018, doi: 10.1109/TBME.2017.2752701.

[19] M. Niemeijer, M. D. Abràmoff, and B. Van Ginneken, "Information fusion for diabetic retinopathy CAD in digital color fundus photographs," *IEEE Trans. Med. Imaging*, vol. 28, no. 5, pp. 775–785, 2009, doi: 10.1109/TMI.2008.2012029.

[20] R. Casanova, S. Saldana, E. Y. Chew, R. P. Danis, C. M. Greven, and W. T. Ambrosius, "Application of Random Forests Methods to Diabetic Retinopathy Classification Analyses," *PLoS One*, vol. 9, no. 6, p. e98587, Jun. 2014, doi: 10.1371/JOURNAL.PONE.0098587.

[21] S. Sanromà, A. Moreno, A. Valls, P. Romero, S. De La Riva, and R. Sagarra, "Assessment of diabetic retinopathy risk with random forests," *ESANN 2016 - 24th Eur. Symp. Artif. Neural Networks*, no. April, pp. 313–318, 2016.

[22] A. Herliana, T. Arifin, S. Susanti, and A. B. Hikmah, "Feature Selection of Diabetic Retinopathy Disease Using Particle Swarm Optimization and Neural Network," *2018 6th Int. Conf. Cyber IT Serv. Manag. CITSM 2018*, no. Citsm, pp. 2016–2019, 2019, doi: 10.1109/CITSM.2018.8674295.

[23] M. Memon, M. M., Jawaid, M. M., Narejo, S., & Rathi, "Computer-Assisted Framework for Automatic Detection of Structural Hand Deformities," *J. Hunan Univ. Nat. Sci.*, vol. 48, no. 10, 2021, Accessed: May 22, 2024. [Online]. Available: http://jonuns.com/index.php/journal/article/view/826

[24] T. Shanthi and R. S. Sabeenian, "Modified Alexnet architecture for classification of diabetic retinopathy images," *Comput. Electr. Eng.*, vol. 76, pp. 56–64, Jun. 2019, doi: 10.1016/J.COMPELECENG.2019.03.004.

[25] A. R. Wahab Sait, "A Lightweight Diabetic Retinopathy Detection Model Using a Deep-Learning Technique," *Diagnostics 2023, Vol. 13, Page 3120*, vol. 13, no. 19, p. 3120, Oct. 2023, doi: 10.3390/DIAGNOSTICS13193120.